Axially Moving Materials with Granular Microstructure

Nima Nejadsadeghi[1] and Anil Misra[2*]

[1]Mechanical Engineering Department,
University of Kansas, 1530 W 15th Street, Learned Hall, Lawrence, KS 66047-7609
[2]Civil, Environmental and Architectural Engineering Department,
University of Kansas, 1530 W 15th Street, Learned Hall, Lawrence, KS 66045-7609.
*corresponding author: Ph: (785) 864-1750, Fax: (785) 864-5631, Email: amisra@ku.edu

International Journal of Mechanical Sciences

Abstract

The mechanics of axially moving media is significant because of their broad engineering applications. In many engineering applications, it is beneficial to understand the dynamical material response from a microstructural viewpoint. Here we focus upon wave propagation in axially moving materials with granular microstructure. To this end, the granular micromechanics approach is utilized since the resulting continuum model is known to predict wave dispersion. To consider axially moving materials, this approach is enhanced to account for the axial velocity using an Eulerian description of the system accounting for convective terms in the material derivatives and utilizing variational approach. The dispersive behavior of axially moving 1D materials are then derived and compared with the dispersive behavior of non-moving materials. In the absence of microstructure, the axially moving material model simplifies to published literature and shows non-dispersive non-symmetric forward and backward waves. In the case of axially moving materials with granular microstructure, the model predicts dispersive non-symmetric waves. In this case, there are two acoustic and two optical wave branches. Axial velocity leads to narrowing and widening in the frequency band gaps in the forward and backward waves, respectively. Negative group velocity is also observed in certain wavenumber ranges. Clearly, the stopbands created by the axial velocity and the non-symmetric dispersive behavior studied here should be considered in engineering designs for vibration control when the axially moving material possesses granular microstructure. The results presented here can also be used to help obtain parameters needed for axially moving granular metamaterials to be designed for particular applications.

Keywords: axially moving media; granular microstructure; dispersion relation; frequency band gaps; granular metamaterials.

1. Introduction

Due to their engineering importance, axially moving materials have been investigated in a number of previous studies. The interest in these problems have remained high (see for example the review in [1]), with an increasing attention being expended to cases in which the materials possess certain heterogeneities or microstructures (see recent works [2,3]), or undergo complex deformation modes [4,5]. The recent studies on axially moving materials include, but are not limited to, vibration, wave propagation, control and stability analysis of axially moving rods [6,7], cables, belts and strings [1,4,8–17], beams [1,4,5,13–15,18–20], membranes [21], plates [1,3,22], rotating rings [4], and periodic media [2,17]. Interesting application of moving media is found in recently developed 2D graphene sheets [23–25] in which the vibration characteristics [26,27] and stability have been determined to be affected by the axial velocity [28]. Other examples of the applications of axially moving media are aerial tramways, mono-cable ropeways, ski lifts, magnetic and paper tapes, band saw blades, and power transmission chains and belts. These media are considered gyroscopic continua, involving translating and rotating materials [16]. In problems involving such media, a stationary control volume that the material flows through is taken as the domain of study. Although the moving material is typically a solid, moving materials are closely related to flowing fluids than to structural mechanics [29]. For problems involving axially moving materials an Eulerian frame of reference is needed to formulate the problem.

As a large number of materials are granular microstructures, and as technological advancements in additive manufacturing pave the way for production of (granular) metamaterials with desired microstructures for special engineering applications, a need to study the response of moving media with embedded microstructure is warranted. The existence of the microstructural characteristic length comparable to the wavelength of excitation at large frequencies [30], necessitates the inclusion of micro-mechano-morphological aspects of the microstructure in the mathematical models describing moving media's behavior. Note that "large frequencies" do not necessarily mean frequencies in the order of, e.g., Megahertz, as much as microstructure should not always be inferred as microscopic scale. In fact, the largeness of the frequency is conceived with regards to the material and geometrical properties of the system of interest. In cases where

microstructure exists, the classical wave equation for elastic materials in the form of a hyperbolic partial differential equation needs extra terms contributing to the effects of the micro-mechano-morphology and inertia of the axially moving medium. The microstructural effect of granular materials on their dispersive behavior is known to be responsible for the emergence of frequency band gaps, as has been shown, along with the external electric field effect on the tunability of such band gaps, in [31–33].

Unlike the experiments performed on axially moving media in the literature (see, for example, [8–11,18,19]), the involvedness of evaluating parameters in experiments related to materials with granular microstructure is typically intractable and experimental approaches have difficulty in providing an exhaustive examination of the behavior of the materials incorporating granular microstructure. Therefore, as the first step to understanding the dynamic behavior of axially moving granular materials, a theoretical approach has been adopted and realized through longitudinal elastic wave propagation analysis in an axially moving 1D granular continuum in the present paper. With respect to the theoretical modeling of 1D vibrations accounting for higher-order strain-gradient elasticity, we note the recent works focusing on the exact analytical and asymptotic solutions of boundary-value problems of rods [34,35]. Considering a 1D problem to study simplifies the mathematics involved, yet makes it possible to qualitatively describe the phenomenon. Doing so, the granular micromechanics approach described in [33,36] is utilized to investigate the dispersive behavior of axially moving media with granular microstructure. In this method, a collection of grains interacting via different grain-pair mechanisms is modeled as the material representative volume element (RVE), where considering the mean behavior of grain pairs results in the treatment of the problem in statistical sense [37]. Such method is well suited for continuum description of random granular media. An understanding of the effects of the axial velocity and material properties of the moving material with granular microstructure on its dispersive behavior will be beneficial for designing new (meta)materials with desired vibration mitigation objectives as well as indispensable for understanding the stability behavior of existing natural materials with granular microstructure.

The rest of the paper is ordered as follows. An outline of the granular micromechanics theory is delivered in section 2, where we present the kinematics involved in the model and the variational approach utilized to obtain the governing equations of motion. Section 3 is devoted to the study

of the dispersive behavior of an axially moving 1D continuum experiencing longitudinal elastic deformation waves. Studying a 1D continuum model is to avoid complexities, and yet be able to interpret the effects of the axial velocity. In Section 4, simpler forms of the problem reducing to published literature are provided, and analyzed first. Thereafter, the general problem involving axially moving 1D continuum with granular microstructure is investigated in terms of wave propagation characteristics. Finally, section 5 summarizes the paper and provides concluding remarks.

2. Mathematical Model for Axially Moving Materials with Granular Microstructure

Granular micromechanics approach describes the continuum measures based upon the micro-mechanics of grain-scale motions. Therefore, the collective behavior of grain-pair interactions is related to the macro-scale continuum description of the material. Such a relationship identifies the volume average of the interaction energies in the scale of individual grains with the macro-scale deformation energy density. In what follows, the continuum modeling framework of granular micromechanics approach is briefly presented. The reader is referred to the reference [33] for more detailed derivations.

Each material point in the continuum model is considered to be a representative volume element (RVE), as shown in Fig. 1. Now Let **x** be the global or macro-scale coordinate system for the continuum. Further, let **x'** be the local or micro-scale coordinate system, parallel to the macro-scale coordinate system **x** and attached to the center of mass of the material point P. Such micro-scale coordinate system can distinguish the grains inside the RVE. The displacement of the centroids of the grains are, therefore, described as

$$\phi_i = \phi_i(x_j, x'_j, t)\,, \tag{1}$$

where ϕ_i denotes the displacement of grain centroids. Now consider the displacement of the grain p centroid, denoted by ϕ_i^{p}, as defined in [33]. The grain p resides in the continuum material point (the RVE). Consider the neighboring grain n of grain p. One can write the displacement of the centroid of grain n, ϕ_i^{n}, using Taylor series expansion about the displacement of grain p centroid.

Keeping up to the quadratic term in the expansion, and denoting the difference between ϕ_i^{p} and ϕ_i^{n} as δ_i^{np}, results in

$$\delta_i^{\mathrm{np}} = \phi_i^{\mathrm{p}} - \phi_i^{\mathrm{n}} = \phi_{i,j}^{\mathrm{n}} l_j + \frac{1}{2}\phi_{i,jk}^{\mathrm{n}} l_j l_k . \tag{2}$$

In Eq. (2), l_j is the vector joining the centroids of n and p, and the tensor product $l_j l_k$ $(=J_{jk})$ is a geometry moment tensor. The differentiation in Eq. (2) is with respect to the micro-scale coordinate system. Henceforward, differentiation with respect to the spatial coordinate systems is denoted by a comma in the subscript, and over-dots on the parameters express differentiation with respect to time. Moreover, repeated indices in the subscript follow the summation convention unless noted otherwise. The relative rotation of two neighboring grains, n and p, denoted by θ_i^{u} is found similarly as [33]

$$\theta_i^{\mathrm{u}} = e_{jki}\phi_{k,jp} l_p , \tag{3}$$

where e_{ijk} is the permutation symbol. In Eq. (3), the differentiation is with respect to the micro-scale coordinate system. The decomposition of the displacement gradient field can be introduced as [33,36,38]

$$\psi_{ij} = \phi_{i,j} = \bar{\phi}_{i,j} - \gamma_{ij} , \tag{4}$$

where ψ_{ij} is the micro-scale displacement gradient within the RVE, $\bar{\phi}_{i,j}$ is the macro-scale displacement gradient and is constant in a material point, and γ_{ij} is the relative deformation due to the fluctuations of the micro-displacement of the grains inside the RVE. Note that the micro-scale deformation measure ψ_{ij} is homogenous within the material point and is only a function of the macro-scale coordinate system. Using Eq. (4), the relative displacement of grains p and n is written as

$$\delta_i^{\mathrm{np}} = \bar{\phi}_{i,j} l_j - \gamma_{ij} l_j + \frac{1}{2}\phi_{i,jk} l_j l_k = \delta_i^{\mathrm{M}} - \delta_i^{\mathrm{m}} + \delta_i^{\mathrm{g}} , \tag{5}$$

where

$$\delta_i^{\mathrm{M}} = \bar{\phi}_{i,j} l_j, \quad \delta_i^{\mathrm{m}} = \gamma_{ij} l_j, \quad \delta_i^{\mathrm{g}} = \frac{1}{2} \phi_{i,jk} l_j l_k . \tag{6}$$

In Eq. (6), δ_i^{M} is related to the macro-scale (average) displacement gradient, $\bar{\phi}_{i,j}$, δ_i^{m} is related to the gradients of the fluctuation in grain displacement, γ_{ij}, and δ_i^{g} is due to the second gradient term, $\phi_{i,jk}$, which is same as the gradient of the relative deformation, $\gamma_{ij,k}$.

Macro-scale deformation energy density, W, of the granular medium is considered to be a function of the macro-scale kinematic measures, and reads

$$W = W\left(\bar{\phi}_{(i,j)}, \gamma_{ij}, \phi_{i,jk}\right), \tag{7}$$

where $\bar{\phi}_{(i,j)}$ is the symmetric part of the macro-scale displacement gradient. Conjugates to the macro-scale kinematic measures, are the macro-scale stress components written as

$$\tau_{ij} = \frac{\partial W}{\partial \bar{\phi}_{(i,j)}} = \frac{\partial W}{\partial \varepsilon_{ij}}, \quad \sigma_{ij} = \frac{\partial W}{\partial \gamma_{ij}}, \quad \mu_{ijk} = \frac{\partial W}{\partial \gamma_{ij,k}}, \tag{8}$$

where τ_{ij}, σ_{ij}, and μ_{ijk} are Cauchy stress, relative stress, and double stress, respectively. Macro-scale deformation energy density can also be written in terms of micro-scale deformation energy density. Micro-scale deformation energy for the α^{th} interacting pair can be defined as $W^{\alpha}\left(\delta_i^{\alpha\mathrm{M}}, \delta_i^{\alpha\mathrm{m}}, \delta_i^{\alpha\mathrm{g}}, \theta_i^{\alpha\mathrm{u}}\right)$. Therefore, the overall energy density of the RVE is given as

$$W = \frac{1}{V'} \sum_{\alpha} W^{\alpha}\left(\delta_i^{\alpha\mathrm{M}}, \delta_i^{\alpha\mathrm{m}}, \delta_i^{\alpha\mathrm{g}}, \theta_i^{\alpha\mathrm{u}}\right). \tag{9}$$

In Eq. (9), V' is the volume of the RVE. The intergranular forces, $f_i^{\alpha\mathrm{M}}, f_i^{\alpha\mathrm{m}}, f_i^{\alpha\mathrm{g}}$, and moment, $m_i^{\alpha\mathrm{u}}$, conjugates to the kinematic measures in Eq. (9) are introduced as

$$\frac{\partial W}{\partial \delta_i^{\alpha\zeta}} = f_i^{\alpha\zeta}; \quad \zeta=\mathrm{M,m,g}, \qquad \frac{\partial W}{\partial \theta_i^{\alpha\mathrm{u}}} = m_i^{\alpha\mathrm{u}} . \tag{10}$$

Substitution of Eq. (9) in Eq. (8), and utilizing Eq. (6) and Eq. (10), results in the equations relating macro-scale stress measures to the grain-pair forces and moments, branch vectors and geometry moment tensors as follows [33]

$$\tau_{ij}=\frac{1}{V'}\sum_{\alpha} f_i^{\alpha \mathrm{M}} l_j^{\alpha}, \quad \sigma_{ij}=\frac{1}{V'}\sum_{\alpha} f_i^{\alpha \mathrm{m}} l_j^{\alpha}, \quad \mu_{ijk}=\frac{1}{V'}\left(\sum_{\alpha} f_i^{\alpha \mathrm{g}} J_{jk}^{\alpha}+\sum_{\alpha} m_l^{\alpha \mathrm{u}} e_{jil} l_k^{\alpha}\right). \tag{11}$$

A local coordinate system for each grain pair can be defined. The grain-pair forces and moments, as well as displacement and rotation vectors can subsequently be decomposed in normal and tangential components. Considering a quadratic form for W^{α} results in the macro-scale constitutive relationships in the macro-scale coordinate system as follows [33]

$$\tau_{ij}=C_{ijkl}^{\mathrm{M}}\varepsilon_{kl}, \quad \sigma_{ij}=C_{ijkl}^{\mathrm{m}}\gamma_{kl}, \quad \mu_{ijk}=\left(A_{ijklmn}^{\mathrm{g}}+A_{ijklmn}^{\mathrm{u}}\right)\phi_{l,mn}, \tag{12}$$

where C_{ijkl}^{M} and C_{ijkl}^{m} are fourth rank tensors, and A_{ijklmn}^{g} and A_{ijklmn}^{u} are tensors of rank six, defined as (refer to [33] for more details)

$$\begin{aligned} &C_{ijkl}^{\mathrm{M}}=\frac{1}{V'}\sum_{\alpha} K_{ik}^{\mathrm{M}} l_l^{\alpha} l_j^{\alpha}, \quad C_{ijkl}^{\mathrm{m}}=\frac{1}{V'}\sum_{\alpha} K_{ik}^{\mathrm{m}} l_l^{\alpha} l_j^{\alpha}, \\ &A_{ijklmn}^{\mathrm{g}}=\frac{1}{V'}\sum_{\alpha} K_{il}^{\mathrm{g}} J_{mn}^{\alpha} J_{jk}^{\alpha}, \quad A_{ijklmn}^{\mathrm{u}}=\frac{1}{V'}\sum_{\alpha} G_{pq}^{\mathrm{u}} e_{mlq} e_{jip} l_k^{\alpha} l_n^{\alpha}. \end{aligned} \tag{13}$$

In Eq. (13), $\mathbf{K}^{\mathrm{M}}$, $\mathbf{K}^{\mathrm{m}}$, $\mathbf{K}^{\mathrm{g}}$, and $\mathbf{G}^{\mathrm{u}}$ denote average, fluctuation, second gradient, and rotational inter-granular stiffness matrices. We note that, in general, grain-pair interaction is nonlinear and includes dissipation. However, for small deformations (small amplitude of vibration) a quadratic form of grain-pair deformation energy based on the micro-scale kinematic measures is considered valid.

In what follows, we will derive the equations of motion for a moving granular medium observed from a stationary reference frame. The granular medium is assumed to move with a known constant velocity **v**, a vector with components in directions of X_1, X_2, and X_3, respectively, with **X** being the stationary frame of reference. Although the axially moving continua are non-conservative with respect to the fact that the total energy is not generally constant, and the collection of material points establishing the material inside the control volume changes with time, the standard form of Hamilton's principle can still be applied to derive the equations of motion, provided that the end supports are fixed [12,39].

The variation of macro-scale deformation energy density, using Eq. (4) and Eq. (8), can be written as

$$\delta W = \tau_{ij}\delta\varepsilon_{ij} + \sigma_{ij}\delta\gamma_{ij} + \mu_{ijk}\delta\phi_{i,jk} = \tau_{ij}\delta\bar{\phi}_{(i,j)} + \sigma_{ij}\left(\delta\bar{\phi}_{(i,j)} - \delta\phi_{i,j}\right) + \mu_{ijk}\delta\phi_{i,jk}\,. \tag{14}$$

Leibniz differentiation rule can be applied to Eq. (14), resulting

$$\delta W = \left[\left(\tau_{ij} + \sigma_{ij}\right)\delta\bar{\phi}_i\right]_{,j} - \left(\tau_{ij} + \sigma_{ij}\right)_{,j}\delta\bar{\phi}_i - \sigma_{ij}\delta\psi_{ij} + \left(\mu_{ijk}\delta\psi_{ij}\right)_{,k} - \mu_{ijk,k}\delta\psi_{ij}\,. \tag{15}$$

Defining $\tilde{V}$ as the total macro-scale deformation energy, its variation is obtained utilizing Gauss's divergence theorem and Eq. (15) as

$$\delta\tilde{V} \quad \left(\tau_{ij} + \sigma_{ij}\right)_{,j}\delta\bar{\phi}_i dV - \int_V\left(\mu_{ijk,k} + \sigma_{ij}\right)\delta\psi_{ij}dV + \int_S\left(\tau_{ij} + \sigma_{ij}\right)n_j\delta\bar{\phi}_i dS + \int_S\mu_{ijk}n_k\delta\psi_{ij}dS\,. \tag{16}$$

With regards to Eq. (16), the following form for the variation of total external work is considered

$$\delta\tilde{V} \quad \delta\bar{\phi}_i dV + \int_V\Phi_{ij}\delta\psi_{ij}dV + \int_S t_i\delta\bar{\phi}dS + \int_S T_{ij}\delta\psi_{ij}dS\,, \tag{17}$$

where f_i is the non-contact volumic force per unit volume, t_i is the contact surface force per unit area, Φ_{ij} is the non-contact volumic double force per unit volume, and T_{ij} is the contact double force per unit area.

Non-relativistic kinetic energy density T associated with the material's motion can be written, using the Stokes' (material) derivative

$$\frac{D}{Dt} = \frac{\partial}{\partial t} + v\frac{\partial}{\partial x}, \tag{18}$$

and the defined forms of kinetic energy in [24,32] as

$$T = \frac{1}{V'}\int_{V'}\frac{1}{2}\rho'\left(v_i + \zeta \quad \frac{\partial}{\partial x_j} \quad \frac{\partial}{\partial x_k}\right)\,. \tag{19}$$

In Eq. (19), ρ' is defined as the micro-scale mass density per unit macro-volume. In general, ρ' can be a non-uniform inside the RVE. Here we only consider a constant ρ' in the RVE and the continuum. The macro-scale mass density, ρ, is obtained as

$$\rho = \frac{1}{V'}\int_{V'}\rho' dV' = \frac{\rho'}{V'}\int_{V'}dV' = \rho'\,. \tag{20}$$

Eq. (19), after substituting for ϕ_i and using Eq. (20), can be written as

$$T=\frac{1}{V'}\int_{V'}\frac{1}{2}\rho\left(v_i + \dot{\zeta} \quad \ldots \quad \partial x_j \quad \ldots \quad \partial x_k \right) dV' . \quad (21)$$

Expanding Eq. (21), and noting that the integrals of linear integrands in x_j' vanish, the kinetic energy density takes the form

$$\begin{aligned} T &= \frac{1}{2}\rho\left(\dot{\zeta} \quad \ldots \quad v_m v_j\right) \\ &+\frac{1}{2}\rho d_{jk}\left(\dot{\psi} \quad \ldots \quad +\psi_{ij,l}\psi_{ik,n}v_l v_n\right), \end{aligned} \quad (22)$$

where d_{jk} is

$$d_{jk}=\frac{1}{V'}\int_{V'}x_j'x_k'dV' . \quad (23)$$

We remark here that the expression for the kinetic energy density in Eq. (21) is significantly different from that found in [31–33], which focuses upon non-moving granular media. In the derived expression Eq. (22), the effect of velocity of the axially moving granular medium is included by considering the Eulerian description of grain and the grain-structure motion. It is notable that the Eq. (22) will simplify to the previously published work if one considers a vanishing axial velocity for non-moving media. In this case, the Eulerian and Lagrangian descriptions of motion give identical results and the kinetic energy density will reduce to $T=\frac{1}{2}\rho\dot{\zeta} \ldots \frac{\ldots}{2} \ldots_{jk}\dot{\psi} \ldots$. In the present derivation, the key aspect is the inclusion of the convective terms in the kinetic energy density expression. These inclusion are two-fold, one due to the classical convective term that will appear as a result of the bulk axial velocity v_i, and the second due to the effect of bulk axial velocity on the micro-motions.

Throughout the paper, we consider a cubic RVE with parallel edges to **x***'* and length of *2d*. In this case, Eq. (23) is written as

$$d_{jk}=\frac{1}{3}d^2\delta_{jk} , \quad (24)$$

where δ_{jk} is the Kronecker delta. The total kinetic energy $\tilde{T}$ is written as

$$\tilde{T} \qquad . \tag{25}$$

Using Eq. (22) and Eq. (25), and integrating by parts with the assumption that the values of $\bar{\phi}_j$ and ψ_{ij} are known at $t = t_0, t_1$, the variational of the kinetic energy functional is

$$\begin{aligned}
&\delta\int_{t_0}^{t_1}\tilde{T} \qquad \int_{t_0}\int_V \rho v_i v_j \delta\bar{\phi}_{i,j} dV dt - \int_{t_0}^{t_1}\int_V \rho(\quad) \qquad \int_{t_0}\int_V \qquad \\
&-\int_{t_0}^{t_1}\int_V \rho v_j(\quad) \qquad + \int_{t_0}^{t_1}\int_V \rho v_m v_j \bar{\phi}_{i,m}\delta\bar{\phi}_{i,j} dV dt - \int_{t_0}^{t_1}\int_V \frac{1}{3}\rho d^2(\quad) \qquad dV dt \\
&+\int_{t_0}^{t_1}\int_V \frac{1}{3}\rho d^2 v_m(\quad) \qquad \int_{t_0}^{t_1}\int \qquad dt + \int_{t_0}^{t_1}\int_V \frac{1}{3}\rho d^2 v_m v_n \psi_{ij,m}\delta\psi_{ij,n} dV dt.
\end{aligned} \tag{26}$$

Using Leibniz differentiation rule, we can write for the integrands of the first, third, fifth, seventh and the ninth terms on the right hand side of Eq. (26),

$$\begin{aligned}
&\rho v_i v_j \delta\bar{\phi}_{i,j} = \left(\rho v_i v_j \delta\bar{\phi}_i\right)_{,j}, \\
&\rho v_j(\quad) \qquad \qquad \qquad \qquad \qquad \\
&\rho v_m v_j \bar{\phi}_{i,m}\delta\bar{\phi}_{i,j} = \left(\rho v_m v_j \bar{\phi}_{i,m}\delta\bar{\phi}_i\right)_{,j} - \rho v_m v_j \bar{\phi}_{i,mj}\delta\bar{\phi}_i, \\
&\frac{1}{3}\rho d^2 v_m(\quad) \qquad \qquad \qquad \qquad \\
&\frac{1}{3}\rho d^2 v_m v_n \psi_{ij,m}\delta\psi_{ij,n} = \left(\frac{1}{3}\rho d^2 v_m v_n \psi_{ij,m}\delta\psi_{ij}\right)_{,n} - \frac{1}{3}\rho d^2 v_m v_n \psi_{ij,mn}\delta\psi_{ij}.
\end{aligned} \tag{27}$$

Gauss's divergence theorem can now be applied to give, for the first, third, fifth, seventh and the ninth terms on the right hand side of Eq. (26), using Eq. (27),

$$\int_{t_0}^{t_1}\int_V \rho v_i v_j \delta\bar{\phi}_{i,j} dVdt = \int_{t_0}^{t_1}\int_S \rho v_i v_j n_j \delta\bar{\phi}_i dSdt,$$

$$\int_{t_0}^{t_1}\int_V \rho v_j \dot{\varsigma} \ldots$$

$$\int_{t_0}^{t_1}\int_V \rho v_m v_j \bar{\phi}_{i,m} \delta\bar{\phi}_{i,j} dVdt = \int_{t_0}^{t_1}\int_S \rho v_m v_j \bar{\phi}_{i,m} n_j \delta\bar{\phi}_i dSdt - \int_{t_0}^{t_1}\int_V \rho v_m v_j \bar{\phi}_{i,mj} \delta\bar{\phi}_i dVdt,$$

$$\int_{t_0}^{t_1}\int_V \frac{1}{3}\rho d^2 v_m \dot{\psi}\ldots_j \delta\psi_{ij,m} dVdt = \int_{t_0}^{t_1}\int_S \frac{1}{3}\rho d^2 v_m \dot{\psi}\ldots$$

$$\int_{t_0}^{t_1}\int_V \frac{1}{3}\rho d^2 v_m v_n \psi_{ij,m} \delta\psi_{ij,n} dVdt = \int_{t_0}^{t_1}\int_S \frac{1}{3}\rho d^2 v_m v_n \psi_{ij,m} n_n \delta\psi_{ij} dSdt - \int_{t_0}^{t_1}\int_V \frac{1}{3}\rho d^2 v_m v_n \psi_{ij,mn} \delta\psi_{ij} dVdt.$$

(28)

Governing equations of motion are derived using Hamilton's principle, written as

$$\delta\int_{t_0}^{t_1}\left(\tilde{T} \ldots\right. \tag{29}$$

Substituting Eq. (16), Eq. (17), and Eq. (26) in Eq. (29), and using Eq. (28), result in the balance equations

$$\left(\tau_{ij}+\sigma_{ij}\right)_{,j} + f_i - 2\rho v_j \dot{\varsigma}\ldots$$

$$\mu_{ijk,k} + \sigma_{ij} + \Phi_{ij} - \frac{2}{3}\rho d^2 v_m \dot{\psi}\ldots \tag{30}$$

Moreover, the advantage of the variational approach is that we can clearly define the boundary conditions. The two natural boundary conditions given in terms of the stress measures are

$$\left(\tau_{ij}+\sigma_{ij} - \rho v_i v_j - \rho v_j \dot{\varsigma}\ldots \bar{\varsigma}_{i,m}\right) n_j = t_i,$$

$$\left(\mu_{ijk} - \frac{1}{3}\rho d^2 v_k \dot{\psi}\ldots v_m v_k \psi_{ij,m}\right) n_k = T_{ij}. \tag{31}$$

Finally, displacement equations of motion can be derived, using the constitutive equations of Eq. (12) in Eq. (30). Considering null volumic forces and volumic double forces, the displacement equations of motion are

$$\left(C^{\mathrm{M}}_{ijkl} + C^{\mathrm{m}}_{ijkl}\right)\bar{\phi}_{k,lj} - C^{\mathrm{m}}_{ijkl}\psi_{kl,j} - 2\rho v_j \dot{\varsigma}\ldots$$

$$\left(A^{\mathrm{g}}_{ijklmn} + A^{\mathrm{u}}_{ijklmn}\right)\psi_{lm,nk} + C^{\mathrm{m}}_{ijkl}\bar{\phi}_{k,l} - C^{\mathrm{m}}_{ijkl}\psi_{kl} - \frac{2}{3}\rho d^2 v_m \dot{\psi}\ldots \tag{32}$$

3. Dispersion analysis in axially moving 1D continuum

In what follows, we consider the longitudinal wave propagating along X_1 axis in a one dimensional infinite continuum moving with velocity v_1 in X_1 direction between two fixed ends. A schematic of the general problem has been shown in Fig. 2. A 1D homogenous continuum can be non-homogenous in the RVE in terms of micro-scale mass density and grain-pair interactions. Fig. 2 depicts the former, while the latter is rather difficult to picturize. Our focus in this section is along the assumptions made to derive Eq. (32), and therefore we assume a constant micro-scale mass density. Therefore, the inhomogeneity only comes from grain-pair interactions within the RVE. For brevity, the subscript 1 will be dropped in the following equations. The displacement equations of motion in this case are

$$\begin{aligned} &(P+Q)\bar{\phi}_{,xx} - Q\psi_{,x} - 2\rho v\dot{\psi}_{,x} = \rho\ddot{\bar{\phi}} \\ &R\psi_{,xx} + Q\bar{\phi}_{,x} - Q\psi - 2Iv\dot{\psi} = I\ddot{\psi} \end{aligned} \tag{33}$$

where the symbols *P, Q, R*, and *I* have been used for conciseness, and have the values of C^{M}_{1111}, C^{m}_{1111}, $A^{\mathrm{g}}_{111111} + A^{\mathrm{u}}_{111111}$ and $\frac{1}{3}\rho d^2$, respectively. Eq. (33) are coupled partial differential equations that describe axial deformations of the 1D continuum fragment confined within the shown dashed boundaries in Fig. 2. As discussed before, while the material is moving, the control volume is kept constant. The dashed boundary is assumed to be sufficiently large that the waves do not reach the boundaries, i.e., reflection of the waves is neglected [2]. This assumption has been taken to facilitate the comparison between the dispersive behavior of non-moving infinite 1D continuum [31,32] and the current problem. The convective acceleration terms in Eq. (33), i.e. $2v\dot{\psi}_{,x}$ and $2v\dot{\psi}$, (referred as skew-symmetric, gyroscopic, or with analogy to [12] Coriolis) may result in complex modes with non-constant phase in the free motion analysis [14]. The acceleration terms $\ddot{\bar{\phi}}$ and $\ddot{\psi}$ are called local accelerations, while $v^2\bar{\phi}_{,xx}$ and $v^2\psi_{,xx}$ are centripetal components.

For a sufficiently large span length of the control volume, the solution is represented as d'Alembert waves by assuming harmonic solutions for both position x and time t [12].

Considering the solutions in Eq. (33) to be plane harmonic waves [31,32,38] results in oscillatory motion in both time and spatial coordinate, written as

$$\bar{\phi} = \mathrm{Re}\left(A\mathrm{i}\mathrm{e}^{\mathrm{i}(kx-\omega t)} \right), \quad \psi = \mathrm{Re}\left(B\mathrm{e}^{\mathrm{i}(kx-\omega t)} \right), \tag{34}$$

where k is the wavenumber, ω is the angular frequency, Ai and B are the complex amplitudes of the macro-displacement and micro-displacement-gradient, respectively, and $\mathrm{i}^2 = -1$. Denoting wavelength by λ, the relation between the wavenumber and wavelength is expressed as

$$k = \frac{2\pi}{\lambda}, \tag{35}$$

and the frequency f is related to ω with the expression

$$\omega = 2\pi f. \tag{36}$$

In what follows, for brevity, the term "frequency" is used for ω instead of the term "angular frequency". By substituting the solutions in Eq. (34) in Eq. (33), we have the system of linear equations in the matrix form

$$\begin{bmatrix} c_0^2 k^2 - v^2 k^2 + 2v\omega k & c_A^2 k \\ \dfrac{k}{p^2} & c_1^2 k^2 - v^2 k^2 + \dfrac{1}{p^2} + 2v\omega k \end{bmatrix} \begin{bmatrix} A \\ B \end{bmatrix} = \omega^2 \begin{bmatrix} A \\ B \end{bmatrix}, \tag{37}$$

where we have introduced the velocities c_0, c_1, c_A, and characteristic time p as [30–32]

$$c_0^2 = \frac{P+Q}{\rho}, \quad c_1^2 = \frac{R}{I}, \quad c_A^2 = \frac{Q}{\rho}, \quad p^2 = \frac{I}{Q}. \tag{38}$$

In order to obtain the dimensionless form of the equations, we define, the dimensionless wavenumber and frequency as

$$\xi = pc_0 k, \qquad \eta = p\omega, \tag{39}$$

and dimensionless velocities as

$$\gamma_A = \frac{c_A}{c_0} = \sqrt{\frac{Q}{P+Q}}, \quad \gamma_1 = \frac{c_1}{c_0} = \sqrt{\frac{R}{P+Q}}\sqrt{\frac{\rho}{I}}, \quad \hat{v} = \frac{v}{c_0}. \tag{40}$$

Utilizing the dimensionless parameters defined in Eq. (39) and Eq. (40), we obtain the following solutions for the dimensionless frequency

$$\begin{aligned}
\eta &= \hat{v}\xi + \frac{1}{2}\sqrt{2\gamma_1^2\xi^2 + 2\xi^2 + 2\sqrt{\gamma_1^4\xi^4 - 2\gamma_1^2\xi^4 + 2\gamma_1^2\xi^2 + \xi^4 + 4\gamma_A^2\xi^2 - 2\xi^2 + 1} + 2}, \\
\eta &= \hat{v}\xi - \frac{1}{2}\sqrt{2\gamma_1^2\xi^2 + 2\xi^2 + 2\sqrt{\gamma_1^4\xi^4 - 2\gamma_1^2\xi^4 + 2\gamma_1^2\xi^2 + \xi^4 + 4\gamma_A^2\xi^2 - 2\xi^2 + 1} + 2}, \\
\eta &= \hat{v}\xi + \frac{1}{2}\sqrt{2\gamma_1^2\xi^2 + 2\xi^2 - 2\sqrt{\gamma_1^4\xi^4 - 2\gamma_1^2\xi^4 + 2\gamma_1^2\xi^2 + \xi^4 + 4\gamma_A^2\xi^2 - 2\xi^2 + 1} + 2}, \\
\eta &= \hat{v}\xi - \frac{1}{2}\sqrt{2\gamma_1^2\xi^2 + 2\xi^2 - 2\sqrt{\gamma_1^4\xi^4 - 2\gamma_1^2\xi^4 + 2\gamma_1^2\xi^2 + \xi^4 + 4\gamma_A^2\xi^2 - 2\xi^2 + 1} + 2}.
\end{aligned} \tag{41}$$

Eq. (41) are the most general form of the frequency solutions for the problem at hand.

4. Effects of axial velocity and granular microstructure

Before analyzing these general solutions, we briefly study the simplified forms of the problem. As a special simplified case where the microstructure, and correspondingly the material properties related to microstructure are absent, Eq. (33) can be simplified. Upon substituting plane wave solution form of the left equation in Eq. (34) and nondimensionalizing the axial velocity using the last of Eq. (40), the following dispersion relation is found

$$\left(1-\hat{v}^2\right)k^2 + \frac{2\hat{v}\omega k}{c_0} - \frac{\omega^2}{c_0^2} = 0\,. \tag{42}$$

Eq. (42) is similar to what has been presented in [2], and after solving for ω yields

$$\omega = c_0\left(\hat{v} \pm 1\right)k\,. \tag{43}$$

By multiplying both sides of Eq. (43) by a nonzero characteristic time constant p', the dimensionless form of Eq. (43) is written as

$$\hat{\omega} = \left(\hat{v} \pm 1\right)\hat{k}\,, \tag{44}$$

where

$$\hat{\omega} = p'\omega, \quad \hat{k} = p'c_0 k\,, \tag{45}$$

are the dimensionless frequency and wavenumber, respectively. Eq. (44) shows a non-dispersive non-symmetric behavior in the propagating forward and backward wave branches for an axially moving long thin 1D continuum (also referred to as rod in [2]). Fig. 3 shows the two forward and backward branches for vanishing and non-zero values of $\hat{v}$. Clearly, for the non-moving (stationary) case where $\hat{v}=0$, the dimensionless phase velocity ($\hat{\omega}/\hat{k}$) and dimensionless group velocity ($d\hat{\omega}/d\hat{k}$) of the forward and backward wave branches are equal in magnitude and different in sign, suggesting existence of symmetry in the propagating waves. In this case, the slopes of the wave branches are unity and Eq. (44) simplifies to the dispersion relation of the classical 1D wave and suggests elastic reciprocity in the forward and backward waves.

For the case where $\hat{v}\neq 0$, the effect of axial velocity on the dispersion curve can be analyzed using Eq. (44). In this case, the phase and group velocities (the slopes) for the forward and backward wave branches are $\hat{v}+1$ and $\hat{v}-1$, respectively. This suggests that the effect of axial velocity on the dimensionless phase and group velocity values is observed as a translation by the amount of the dimensionless axial velocity $\hat{v}$. This change in velocities is attributed to a linear momentum bias resulting from the axial velocity $\hat{v}$ [2]. The dimensionless form of the dispersion relation for a non-moving 1D medium based upon classical analysis described as $\hat{\omega}=\pm\hat{k}$ undergoes a shift in frequency by the amount of $\hat{v}\hat{k}$. When the dimensionless axial velocity is less than unity (which corresponds to axial velocity less than the wave velocity in non-moving medium), the phase and group velocities for the forward wave are positive in sign, while those for the backward wave are negative in sign. For the extreme cases, where the dimensionless axial velocity is 1 or greater than 1, the predictions of Eq. (44) are the following. For dimensionless axial velocity $\hat{v}=1$, the backward wave disappears and only one forward wave propagates. The phase (and group) velocity for this forward propagating wave is twice that for the non-moving medium. In this case, the stationary observer on one of the end supports will not experience any vibration. For dimensionless axial velocities larger than unity (corresponding to axial velocities larger than the wave velocity of the non-moving medium), the backward wave flips over the forward side. The stationary observer on the support corresponding to the backward wave will not experience aand vibration, while the observer on the support corresponding to the forward wave will see two wave arrivals. Based on Eq. (44), for any real wavenumber, the frequency is always real, therefore, there is no instability or attenuation for these propagating waves. It is also

notable that in the case of classical analysis, the absence of microstructural effects lead to non-dispersive behavior as both dimensionless phase and group velocities are equal and constant for each forward and backward wave.

For a material with granular microstructure, however, the wave propagation analysis exhibits dispersive behavior, i.e., the wave velocities are functions of wavenumber (or frequency). For vanishing values of axial velocity (stationary case), solutions presented in Eq. (41) take the form [31]

$$\begin{aligned}\eta &= \pm\frac{1}{2}\sqrt{2\gamma_1^2\xi^2+2\xi^2+2\sqrt{\gamma_1^4\xi^4-2\gamma_1^2\xi^4+2\gamma_1^2\xi^2+\xi^4+4\gamma_A^2\xi^2-2\xi^2+1}+2},\\ \eta &= \pm\frac{1}{2}\sqrt{2\gamma_1^2\xi^2+2\xi^2-2\sqrt{\gamma_1^4\xi^4-2\gamma_1^2\xi^4+2\gamma_1^2\xi^2+\xi^4+4\gamma_A^2\xi^2-2\xi^2+1}+2}.\end{aligned} \tag{46}$$

Dispersion curves for two different granular structures for zero axial velocity using Eq. (46) have been plotted in Fig. 4. The material parameters chosen for Fig. 4(a) and Fig. 4(b) are $\gamma_A = 0.7, \gamma_1 = 0.05$, and $\gamma_A = 0.5, \gamma_1 = 0.3$, respectively. These values have been chosen to show two different cases of wave propagation in terms of the existence of stopbands. Note that for a specific granular structure, identification of material parameters can be done, for instance, as has been described in [40]. The frequency solutions in Eq. (46) lead to the emergence of four wave branches in two groups, two forward and two backward waves, with each group having one acoustic and one optical branch. While the acoustic branches start at zero frequency and zero wavenumber, for the optical branches, zero wavenumber produces a dimensionless frequency of unity, meaning that for dimensionless frequencies smaller than unity, there is no optical branch. In this case, the forward and backward waves are symmetrically propagating as their governing equations are different only by a sign. This symmetry in propagating waves can also be attributed to the lack of linear momentum bias in non-moving media. Different grain-pair interactions and/or micro-morphological aspects in the microstructure of the granular material result in different values in stiffness tensors, which consequently lead to different behaviors in the propagation of waves. Two cases wherein one shows frequency band gaps and the other does not, have been exemplified in Fig. 4(a) and Fig. 4(b), respectively. In both cases, corresponding phase and group velocities for each wave branch have the same direction. In other words, for the forward wave branches, phase and group velocities are positive in sign, and for the backward

wave branches, phase and group velocities are all negative in sign. Note that in these cases the frequency solutions are all real, excluding instability or attenuation.

For a nonzero value of the dimensionless axial velocity, $\hat{v}$, however, there exists asymmetry in propagation of the forward and backward wave branches. The asymmetry coming from the axially moving velocity of the medium, along with the microstructural length and inertial effects, brings about interesting observations in wave propagation phenomenon. For the same value of geometrical and mechanical properties of the granular structure studied in Fig. 4(a) and Fig. 4(b), the dispersion curves for $\hat{v} = 0.4$ have been plotted in Fig. 5(a) and Fig. 5(b), respectively, based upon Eq. (41). In this example the dimensionless axial velocity is taken to be 40% (which can be considered somewhat large) of the conventional wave velocity, c_0, such that the trends in the plots are clearly visible.

For the case of Fig. 5(a), a comparison with Fig. 4(a) reveals narrowing and widening in the frequency band gaps in the forward and backward waves, respectively. Of course, the axial velocity in this case is large enough that the stopband for the forward waves has disappeared. As is seen from Fig. 5(a), the symmetry between forward and backward waves is broken. This leads to difference in velocities in the forward and backward acoustic, as well as optical, wave branches. The same effects can also be seen by comparing Fig. 4(b) and Fig. 5(b). In this case, non-existing frequency band gaps in the backward waves in Fig. 4(b) appear for the case of the moving granular medium of Fig. 5(b). This created band gap is "induced" by the axial velocity of the granular medium, and is in contrast to the "inherent" band gap shown by the non-moving granular medium. One remarkable result is that in frequency ranges corresponding to the band gap in the backward waves, the stationary observer on one end support experiences the vibration, while the stationary observer on the other end support does not. Using Eq. (41), for axially moving 1D granular media, the effect of axial velocity on the dimensionless phase and group velocity values is seen to be a translation by the amount of the dimensionless axial velocity $\hat{v}$. This observation is similar to the findings for axially moving 1D continuum without microstructure. Interestingly, the effect of axial velocity on the dispersion curve also follows that of an axially moving 1D material without microstructure, where the frequency solutions undergo a shift by the amount of $\hat{v}\hat{k}$. When increasing the value of the dimensionless axial velocity, $\hat{v}$, the forward waves band gap (if exists) starts disappearing, and the backward waves

band gap (if exist) starts growing (or appearing and growing if it did not exist). As the value of the axial velocity reaches $\hat{v}=1$, Eq. (41) predicts a complete reversal of the backward acoustic branch (in contrast to partial reversal in only certain wavenumbers observed in both cases in Fig. 5 for $\hat{v}=0.4$), meaning that the acoustic branch is not propagated backward. The optical backward branch still starts at a dimensionless frequency of magnitude 1 with negative phase velocity and positive group velocity, but reaches the line $\eta=0$ as its asymptote in large wavenumbers, suggesting that the backward optical branch disappears for large wavenumbers. As the value of the dimensionless axial velocity $\hat{v}$ becomes larger than unity, the backward optical branch starts propagating as a forward wave, and hence, there will be no waves propagating backwards and four wave branches propagating forward. In this case, the stationary receiver on the support corresponding to the backward direction will not experience any vibration.

One other interesting observation from Fig. 5 is the presence of regions (shown in the plots by dash-dotted blocks) in which the sign of the phase and group velocities are different for the particular wave branches. This phenomenon is generally known as negative group velocity (NGV). In the case of NGV, "the peak of the transmitted pulse exits the material before the peak of the incident pulse enters the material" [41]. A consequence of NGV is that the peak of the pulse propagates in the opposite direction. However, energy maintains forward flow [42]. NGV has also been recognized for deformation waves in micro-structured solids with multiple scales [43] and for granular media with negative grain-pair second gradient stiffnesses [31].

5. Summary and conclusions

In this paper, the governing equations of motion for an axially moving material with granular microstructure were derived using Hamilton's Principle. Subsequently, the predicted dispersive behavior of axially moving 1D materials with granular microstructure was explored. The study presented can be summarized as follows: 1) The special simplified case where the micro-scale effect is absent results in asymmetry in the forward and backward propagating waves for non-zero axial velocities, but there is no dispersion as has been reported in the literature. This simplified case considers the medium as a classical Cauchy material resulting in no distinction between phase and group velocities for each forward and backward waves. 2) For a non-moving medium with granular microstructure, there is symmetry in propagating forward and backward

waves, but the behavior is dispersive. There are two wave branches in forward and backward waves, one acoustic and one optical branch, where the optical branches start at dimensionless frequency of magnitude 1 corresponding to zero wavenumber, and the acoustic branches start at dimensionless frequency and wavenumber of zero. 3) For an axially moving medium with granular microstructure, asymmetry in propagation of wave branches for forward and backward waves is observed. Such an asymmetry results in different phase and group velocities for forward and backward waves (for both acoustic and optical branches), narrowing the frequency band gaps range for forward waves, and widening frequency range for which backward stopband exists. 4) In the cases where no band gap is observed for non-moving medium with granular microstructure, it is possible that the stopband is created in the backward propagating waves. This generally means that the backward waves in certain frequencies die exponentially in space, and therefore, there is no vibration sensed by the support receiving the backward waves if the excitation is in the bandgap range. 5) Finally, one notices regions where the phase and group velocities are different in sign, resulting in the phenomenon called negative group velocity.

In what was presented, the effects of material parameters on the dispersive behavior was shown using two examples of granular structures. The macro-mechanical parameters in the studied theory are functions of grain-pair stiffnesses introduced in [33]. For a granular material, one can obtain the macro-mechanical parameters using sufficient experiments with proper boundary conditions, or using numerical techniques such as one described in [40] for a 2D granular material. Such parameters can then be fed into the continuum models to investigate the dispersive behavior of such media, using the approach introduced in this paper. Clearly, the stopbands created by the axial velocity and the non-symmetric dispersive behavior of axially moving granular materials should be considered in engineering design and application, especially when stop-band filtering is of interest. The model presented here can be used to analyze dynamic behavior of materials with granular microstructure when axially moved between two fixed ends. Solution of inverse problems is also possible using granular micromechanics approach. Several recent published works have studied stationary granular metamaterials' behavior where grains interactions can be customized to give preferred dynamic characteristics (see the review paper in [44]). The analysis provided here can be used to obtain parameters needed for the design of granular metamaterial for particular applications of axially moving medium in which vibration control or stopbands over certain frequency range is required. The approach is rich as it can treat

granular metamaterials with periodic RVEs comprising more than one type of grain, and is especially fruitful in treating physics involving axially moving media in which non-local and higher gradient effects are important, e.g., biomedical nanorobotics devices (see for example [20,22]). Further, the axially moving systems comprising granular metamaterials with dielectric properties have the potential to be further tuned for their wave propagation characteristics to give band gaps in desired frequency ranges [32]. The granular micromechanics approach for design and analysis of the mentioned problem is as follows. Requiring a granular metamaterial for a particular application with a desired dispersive behavior, one can find the macro-mechanical parameters leading to the desired behavior, obtaining equalities and inequalities regarding the grain-pair stiffness values. This is possible since the explicit form of the functions are available in the theory of granular micromechanics, providing a complete domain to search for possible solutions. The obtained microstructural parameters can then be realized through additive manufacturing techniques, as for pantographic metamaterials [45-47], to develop a desired granular metamaterial. Such inverse approach to design granular metamaterials using granular micromechanics theory will be pursued in future publications.

Statement of Competing Interest

Authors have no competing interests to declare.

Acknowledgements

This research is supported in part by the United States National Science Foundation grant CMMI -1727433.

References

[1] Marynowski K, Kapitaniak T. Dynamics of axially moving continua. Int J Mech Sci 2014;81:26–41. doi:10.1016/J.IJMECSCI.2014.01.017.

[2] Attarzadeh MA, Nouh M. Elastic wave propagation in moving phononic crystals and correlations with stationary spatiotemporally modulated systems. AIP Adv 2018;8:105302. doi:10.1063/1.5042252.

[3] Liu JJ, Li C, Fan XL, Tong LH. Transverse free vibration and stability of axially moving nanoplates based on nonlocal elasticity theory. Appl Math Model 2017;45:65–84. doi:10.1016/J.APM.2016.12.006.

[4] Lowe RL, Cooley CG. A Newtonian mechanics formulation for the vibration of translating and rotating elastic continua. J Vib Control 2019; 25(10):1639-1652. doi:10.1177/1077546319825675.

[5] Tang Y, Luo E, Yang X. Complex modes and traveling waves in axially moving Timoshenko beams. Appl Math Mech 2018;39:597–608. doi:10.1007/s10483-018-2312-8.

[6] Barakat R. Transverse Vibrations of a Moving Thin Rod. J Acoust Soc Am 1968;43:533–9. doi:10.1121/1.1910862.

[7] Steinboeck A, Baumgart M, Stadler G, Saxinger M, Kugi A. Dynamical Models of Axially Moving Rods with Tensile and Bending Stiffness. IFAC-PapersOnLine 2015;48:598–603. doi:10.1016/J.IFACOL.2015.05.041.

[8] Li Y, Aron D, Rahn CD. Adaptive vibration isolation for axially moving strings: theory and experiment. Automatica 2002;38:379–90. doi:10.1016/S0005-1098(01)00219-9.

[9] Tan CA, Ying S. Active Wave Control of the Axially Moving String: Theory and Experiment. J Sound Vib 2000;236:861–80. doi:10.1006/JSVI.2000.3040.

[10] Michon G, Manin L, Remond D, Dufour R, Parker RG. Parametric Instability of an Axially Moving Belt Subjected to Multifrequency Excitations: Experiments and Analytical Validation. J Appl Mech 2008;75:41004–8.

[11] Pellicano F, Fregolent A, Bertuzzi A, Vestroni F. Primary and Parametric Non-Linear Resonances of a Power Transmission Belt: Experimental and Theoretical Analysis. J Sound Vib 2001;244:669–84. doi:10.1006/JSVI.2000.3488.

[12] Wickert JA, Mote CD. Linear transverse vibration of an axially moving string–particle system. J Acoust Soc Am 1988;84:963–9. doi:10.1121/1.396611.

[13] Wickert JA, Mote CD. On the energetics of axially moving continua. J Acoust Soc Am 1989;85:1365–8. doi:10.1121/1.397418.

[14] Wickert JA, Mote C. D. J. Classical Vibration Analysis of Axially Moving Continua. J Appl Mech 1990;57:738–44.

[15] Vetyukov Y. Non-material finite element modelling of large vibrations of axially moving strings and beams. J Sound Vib 2018;414:299–317. doi:10.1016/j.jsv.2017.11.010.

[16] Chen L-Q. Analysis and Control of Transverse Vibrations of Axially Moving Strings. Appl Mech Rev 2005;58:91–116.

[17] Sorokin VS, Thomsen JJ. Wave propagation in axially moving periodic strings. J Sound Vib 2017;393:133–44. doi:10.1016/j.jsv.2017.01.014.

[18] Yuh J, Young T. Dynamic Modeling of an Axially Moving Beam in Rotation: Simulation and Experiment. J Dyn Syst Meas Control 1991;113:34–40.

[19] Duan Y-C, Wang J-P, Wang J-Q, Liu Y-W, Shao F. Theoretical and experimental study on the transverse vibration properties of an axially moving nested cantilever beam. J Sound Vib 2014;333:2885–97. doi:10.1016/J.JSV.2014.02.021.

[20] Li C. Nonlocal thermo-electro-mechanical coupling vibrations of axially moving piezoelectric nanobeams. Mech Based Des Struct Mach 2017;45:463–78.

[21] Shin C, Kim W, Chung J. Free in-plane vibration of an axially moving membrane. J Sound Vib 2004;272:137–54. doi:10.1016/S0022-460X(03)00323-7.

[22] Li C, Liu JJ, Cheng M, Fan XL. Nonlocal vibrations and stabilities in parametric resonance of axially moving viscoelastic piezoelectric nanoplate subjected to thermo-electro-mechanical forces. Compos Part B Eng 2017;116:153–69.

[23] Gugliuzza A, Politano A, Drioli E. The advent of graphene and other two-dimensional materials in membrane science and technology. Curr Opin Chem Eng 2017;16:78–85. doi:10.1016/J.COCHE.2017.03.003.

[24] Politano A, Argurio P, Di Profio G, Sanna V, Cupolillo A, Chakraborty S, et al. Photothermal Membrane Distillation for Seawater Desalination. Adv Mater 2017;29:1603504. doi:10.1002/adma.201603504.

[25] Politano A, Cupolillo A, Di Profio G, Arafat HA, Chiarello G, Curcio E. When plasmonics meets membrane technology. J Phys Condens Matter 2016;28:363003. doi:10.1088/0953-8984/28/36/363003.

[26] Verre S, Ombres L, Politano A. Evaluation of the Free-Vibration Frequency and the Variation of the Bending Rigidity of Graphene Nanoplates: The Role of the Shape Geometry and Boundary Conditions. J Nanoscience and Nanotechnology 2017;17: 8827-8834. doi:10.1166/jnn.2017.13906.

[27] Politano A, Marino AR, Campi D, Farías D, Miranda R, Chiarello G. Elastic properties of a macroscopic graphene sample from phonon dispersion measurements. Carbon N Y 2012;50:4903–10. doi:10.1016/J.CARBON.2012.06.019.

[28] Arani AG, Haghparast E, BabaAkbar Zarei H. Nonlocal vibration of axially moving graphene sheet resting on orthotropic visco-Pasternak foundation under longitudinal magnetic field. Phys B Condens Matter 2016;495:35–49. doi:10.1016/J.PHYSB.2016.04.039.

[29] Banichuk N, Jeronen J, Neittaanmäki P, Saksa T, Tuovinen T. Mechanics of Moving Materials. Springer International Publishing 2014;207. doi:10.1007/978-3-319-01745-7.

[30] Berezovski A, Engelbrecht J, Salupere A, Tamm K, Peets T, Berezovski M. Dispersive waves in microstructured solids. Int J Solids Struct 2013;50:1981–90. doi:10.1016/J.IJSOLSTR.2013.02.018.

[31] Misra A, Nejadsadeghi N. Longitudinal and transverse elastic waves in 1D granular materials modeled as micromorphic continua. Wave Motion 2019;90:175–95. doi:10.1016/j.wavemoti.2019.05.005.

[32] Nejadsadeghi N, Placidi L, Romeo M, Misra A. Frequency band gaps in dielectric granular metamaterials modulated by electric field. Mech Res Commun 2019;95. doi:10.1016/j.mechrescom.2019.01.006.

[33] Misra A, Poorsolhjouy P. Granular micromechanics based micromorphic model predicts frequency band gaps. Contin Mech Thermodyn 2016;28:215–34. doi:10.1007/s00161-015-0420-y.

[34] Mikhasev G, Avdeichik E, Prikazchikov D. Free vibrations of nonlocally elastic rods. Math Mech Solids 2018;24:1279–93. doi:10.1177/1081286518785942.

[35] Xu X-J, Zheng M-L, Wang X-C. On vibrations of nonlocal rods: Boundary conditions, exact solutions and their asymptotics. Int J Eng Sci 2017;119:217–31. doi:10.1016/J.IJENGSCI.2017.06.025.

[36] Misra A, Poorsolhjouy P. Grain- and macro-scale kinematics for granular micromechanics based small deformation micromorphic continuum model. Mech Res Commun 2017;81:1–6. doi:10.1016/J.MECHRESCOM.2017.01.006.

[37] Misra A, Placidi L, Turco E. Variational Methods for Continuum Models of Granular Materials, 2019, 1–11. doi:10.1007/978-3-662-53605-6_343-1.

[38] Mindlin RD. Micro-structure in linear elasticity. Arch Ration Mech Anal 1964;16:51–78. doi:10.1007/BF00248490.

[39] Thurman AL, Mote C. D. J. Free, Periodic, Nonlinear Oscillation of an Axially Moving Strip. J Appl Mech 1969;36:83–91.

[40] Misra A, Poorsolhjouy P. Identification of higher-order elastic constants for grain assemblies based upon granular micromechanics. Math Mech Complex Syst 2015;3:285–308. doi:10.2140/memocs.2015.3.285.

[41] Gehring GM, Schweinsberg A, Barsi C, Kostinski N, Boyd RW. Observation of Backward Pulse Propagation Through a Medium with a Negative Group Velocity. Science (80-) 2006;312:895 LP-897. doi:10.1126/science.1124524.

[42] Peets T, Kartofelev D, Tamm K, Engelbrecht J. Waves in microstructured solids and negative group velocity. EPL (Europhysics Lett) 2013;103:16001. doi:10.1209/0295-5075/103/16001.

[43] Tamm K, Peets T, Engelbrecht J, Kartofelev D. Negative group velocity in solids. Wave Motion 2017;71:127–38. doi:10.1016/J.WAVEMOTI.2016.04.010.

[44] Kim E, Yang J. Wave propagation in granular metamaterials. Funct Compos Struct

2019;1:12002.

[45] Nejadsadeghi N, De Angelo M, Drobnicki R, Lekszycki T, dell'Isola F, Misra A. Parametric Experimentation on Pantographic Unit Cells Reveals Local Extremum Configuration. Exp Mech 2019:1-13. doi:10.1007/s11340-019-00515-1.

[46] dell'Isola F, Seppecher P, Spagnuolo M, Barchiesi E, Hild F, Lekszycki T, et al. Advances in pantographic structures: design, manufacturing, models, experiments and image analyses. Contin Mech Thermodyn 2019:1-52. doi:10.1007/s00161-019-00806-x.

[47] dell'Isola F, Turco E, Misra A, Vangelatos Z, Grigoropoulos C, Melissinaki V, et al. Force–displacement relationship in micro-metric pantographs: Experiments and numerical simulations. Comptes Rendus Mécanique 2019;347:397–405. doi:10.1016/J.CRME.2019.03.015.

List of Figures

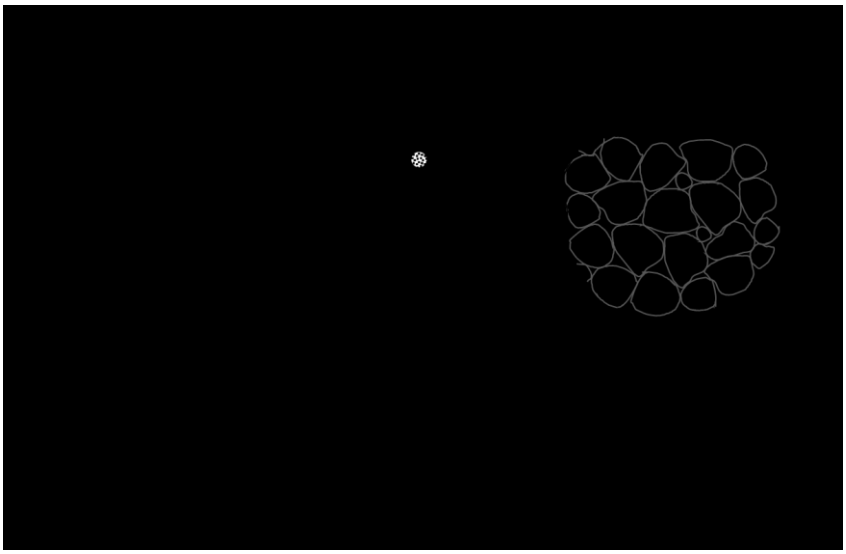

Fig. 1. Schematic of the continuum material point, *P*, and its granular microstructure magnified for visualization, where the *x'* coordinate system is attached to its barycenter.

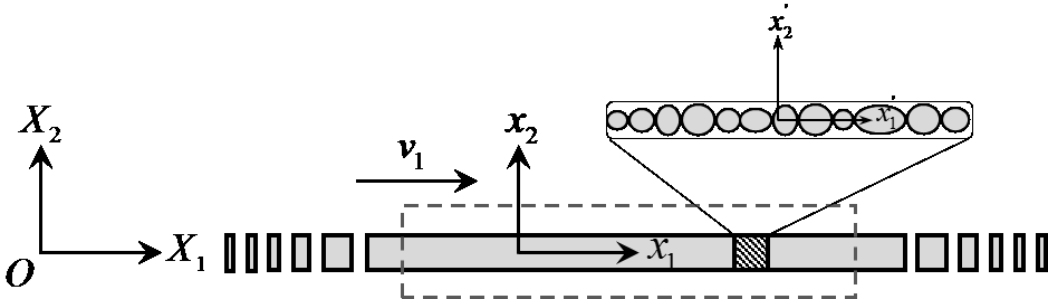

Fig. 2. Schematic of the 1D axially moving media with granular microstructure. A material point in the macro-scale coordinate system is itself a collection of grains that can differ in micro-density, micro-morphology and micro-mechanical properties.

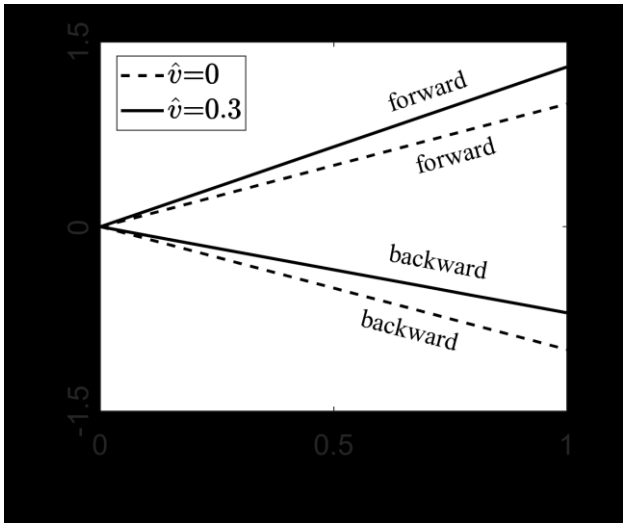

Fig. 3. Dispersion curves for an axially moving 1D continuum without microstructure for two cases of zero and non-zero dimensionless velocities.

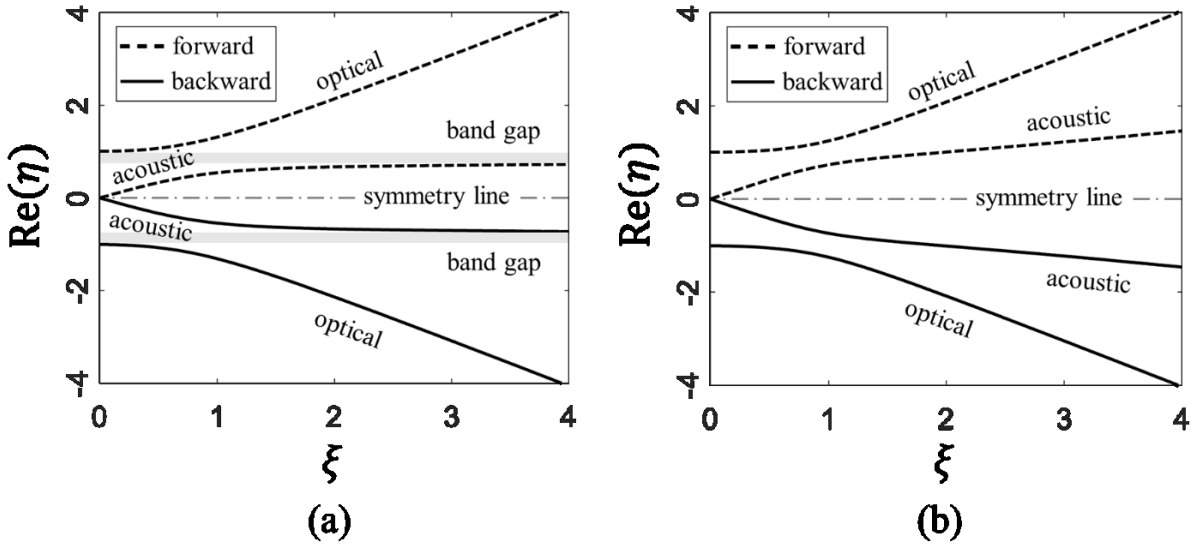

Fig. 4. Dispersion curves for non-moving 1D materials with granular microstructure. (a) The case of $\gamma_A = 0.7, \gamma_1 = 0.05$. (b) The case of $\gamma_A = 0.5, \gamma_1 = 0.3$.

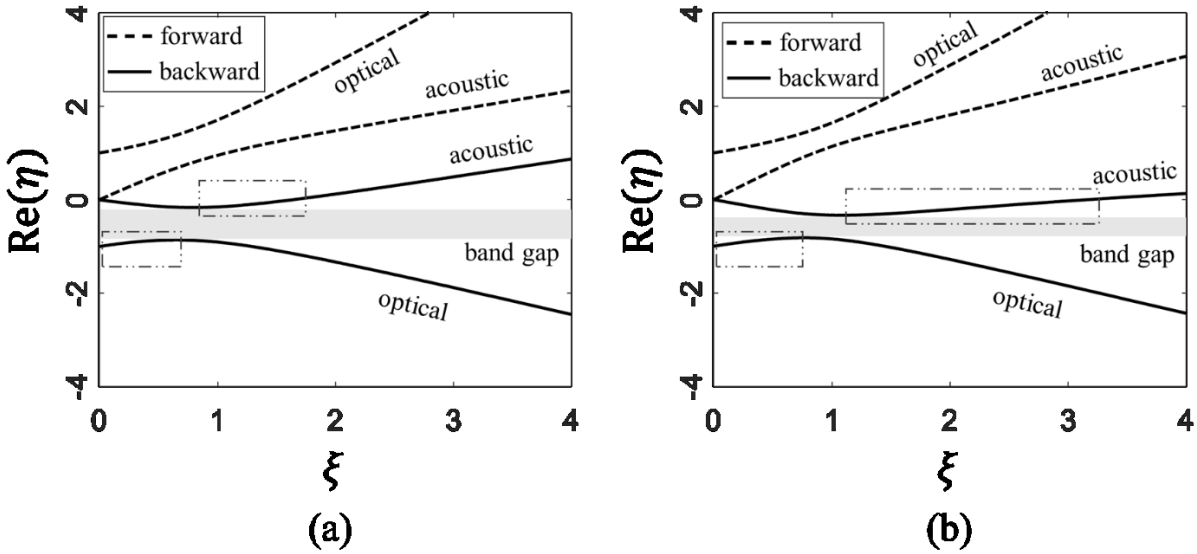

Fig. 5. Dispersion curves for axially moving 1D materials with granular microstructure with dimensionless axial velocity $\hat{v} = 0.4$. (a) The case of $\gamma_A = 0.7, \gamma_1 = 0.05$. (b) The case of $\gamma_A = 0.5, \gamma_1 = 0.3$.